



Numerical analysis with experimental verification of a multi-layer sheet-based funicular glass bridge

Damon BOLHASSANI^{*}, Delaram HASSANLOU^a, Fahimeh YAVARTANOO, Masoud AKBARZADEH^b, Yao LU^b, Joseph R. YOST^c, Jorge H. CHACON^c, Jens SCHNEIDER^d, Philipp A. CHHADEH^d

^{*} ABC Lab, Spitzer School of Architecture, The City College of New York (CCNY), New York, USA

^{*} mbolhassani@ccny.cuny.edu

^a University of Houston

^b Polyhedral Structures Laboratory, University of Pennsylvania

^c Villanova University

^d Technische Universität Darmstadt

Abstract

The sustainability of structural systems and the impact of used construction materials on the environment is an ongoing concern in the construction industry. Multi-layer, sheet-based structures can provide more sustainable solutions for construction mass reduction and its adverse effects. In particular, the use of glass as a structural sheet material has many advantages that are derived from its very high compression strength. While there have been a few attempts regarding the design, fabrication, and manufacturing of multi-layer sheet-based structures, there has not been any comprehensive and detailed numerical analysis and method to show how they can be realistically modeled. Among many other approaches, polyhedral graphic statics (PGS) is an effective technique for designing and constructing spatial sheet-based funicular structures that are dominated by planar faces. In this study, a novel numerical analysis technique has been proposed and implemented for the mechanical behavior of multi-layer sheet-based polyhedral structures, which is based on the Finite Element Method (FEM). This technique aims to simulate the actual physical behavior of such systems, mainly by accurately modeling the interactions between different interfaces and materials. In this research study, a 3m span prototype glass pedestrian bridge designed by PGS is experimentally tested and numerically analyzed. The analysis results of the proposed multi-layer glass sheet-based method are compared and verified by experimental laboratory testing under different loading scenarios and have shown reasonable agreement with measured experimental behavior.

Keywords: Numerical Analysis, Finite Element Method, Funicular Structures, Sheet-Based Structure, Glass Bridge

1. Introduction

The construction of critical infrastructure, such as buildings and bridges, requires a rigorous analysis to ensure both safety and functionality. In contemporary engineering practice, numerical simulations have emerged as essential tools enabling engineers to predict the structural response under various loading conditions. However, the accuracy of these simulations fundamentally depends on the assumptions and simplifications inherent in the modeling process. Therefore, it is crucial to verify the accuracy of numerical simulations through experimental validation.

Experimental tests provide an opportunity to validate the assumptions made during the modeling process, thereby enhancing the accuracy of the simulation results. Additionally, experimental tests provide valuable insight into the behavior of the structure under real-world conditions, which cannot be accu-

rately predicted by numerical simulations alone. By integrating experimental testing alongside numerical analysis, engineers can ensure a comprehensive understanding of the structural response, thereby enhancing the safety and reliability of critical infrastructure projects.

In the past decades, numerous numerical and experimental investigations have been conducted on various civil structures, including steel (Peng and Li [1]), reinforced-concrete (Dashti et al. [2]), and masonry (Bolhassani et al. [3], Yavartanoo and Kang [4]) constructions. However, comparatively little attention has been directed toward multi-layer sheet-based structures.

Multi-layer sheet-based construction is an alternative method for structural and material efficiency and waste reduction in the field of construction and engineering, in which sheet materials are utilized to assemble a multi-layer structure. From a structural perspective, multi-layer sheet-based structures offer the advantage of accommodating diverse loading conditions without excessive weight, as the sheets can provide more load paths across the faces. Additionally, due to sophisticated and efficient structural design procedures, less material would be required for constructing such structures, leading to a greater reduction in the structure's dead load. From the material aspect, sheet-based materials are more accessible, cost-effective, and easier to be fabricated, and manufactured by various techniques (Lu et al. [5], Bolhassani et al. [6]). Specifically, among multi-layer sheet-based structures, design and construction of glass sheets structures has been gaining more popularity among designers and engineers for primary in-plane load-bearing and structural purposes to investigate, instead of merely architectural functionality purposes. (Hussain et al. [7], Lu et al. [5]). Particularly, glass's unique combination of transparency and high compressive strength makes it a logical choice for primary structural roles, especially as an axially loaded compression member in structures designed to utilize compression-dominant force resisting system. Nevertheless, despite the numerous advantages of multi-layer sheet-based structures, the construction of such structures can pose challenges during the design, fabrication, and manufacturing processes. Moreover, numerical modeling of such structures presents unique challenges. For instance, material heterogeneity causes different layers react differently under loading and stress, and complex interlayer interactions demand precise modeling of connections. Furthermore, significant deformations are often encountered during analyses, which amplify these complexities, requiring consideration of geometric nonlinearity that defies simple linear assumptions. These difficulties are further intensified in most cases by limited knowledge about the material properties of different components and the intricate behavior of the overall structure under diverse loading conditions, making the analysis a sophisticated task. While there have been a few efforts regarding design and fabrication of such systems, there has not been accurate and efficient methods proposed for numerical or analytical analysis of these structures.

In this study, a numerical analysis modeling approach for a compression-dominant multi-layer sheet-based funicular compression-dominant glass bridge, recently prototyped by Lu et al. [5] is proposed. The simulation aims to predict the behavior of the glass bridge under various loading conditions. To verify the accuracy of the employed numerical analysis strategies, experimental tests are performed on a real-world model prototype under symmetric loading condition, and the results are compared with those obtained from the numerical simulation.

2. Prototyping

The design, fabrication, and assembly of the glass bridge are concisely summarized in this section building on the documentation by Lu, Cregan, Chhadeh, Seyedahmadian, Bolhassani, Schneider, Yost, and Akbarzadeh [9] and Lu, Seyedahmadian, Chhadeh, Cregan, Bolhassani, Schneider, Yost, Brennan, and Akbarzadeh [5].



Figure 1. A 3m-span bridge prototype made of glass sheets [8].

2.1. Design and Fabrication

The double-layer bridge geometry is designed using PolyFrame [10, 11] (Figure 2a), a Rhino plug-in that implements polyhedral graphic statics (PGS). Then, a detailed 3D model is generated with the help of the handy polyhedral data structure provided by PolyFrame. Each of the thirteen closed polyhedral HGU features top and bottom faces alongside several smaller side faces. The two top and bottom faces are constructed with 9.5mm annealed glass to form the deck plates. The material choice of other smaller side faces is either 9.5mm-thick glass or 21mm-thick acrylic depending on whether they need to accommodate the connection mechanisms with the neighbor modules (Figure 2b, d). This is because the connection mechanism is more difficult to produce in glass than in acrylic. The connection mechanism contains two pocket channels on the opposing side plates and an acrylic locking strip that has a butterfly-shaped section profile. All the glass plates are cut using a 5-axis abrasive water jet cutter, and the acrylic plates are milled using 5-axis milling machines. After cutting is complete, all glass and acrylic plates of an individual module are bonded together using 3M™ Very High Bond (VHB) transparent structural tape, a type of double-sided soft bonding agent (Figure 2c). In the fully assembled bridge, all the top and bottom glass deck plates form two continuous layers and serve as the primary load transfer elements.

2.2. Assembly

Assembly of the whole bridge begins only after the assembly of all thirteen HGUs is completed. Bridge assembly starts with placing some CNC-cut plywood panels on the floor to locate the two steel abutments precisely, which is later secured by two tension ties. The Surlyn sheets are then placed on the steel abutments to avoid steel-to-glass contact. Surlyn sheets are also placed between the HGUs to avoid glass-to-glass contact (Figure 2d). One side of each Surlyn sheet is glued to the corresponding HGU to fix its position using Gorilla™ transparent spray adhesive, which provides strong bonds without adding much construction error.

The choice of the assembly sequence of HGUs has a large impact on the count and locations of butterfly locking connections. It is also critical to note that the final “keystone” HGU may not have any butterfly locking mechanism on its side plates and hence it is more vulnerable to sliding and rotation. For this reason, a unit directly supported by the steel abutment with four sides is selected as the “keystone”.

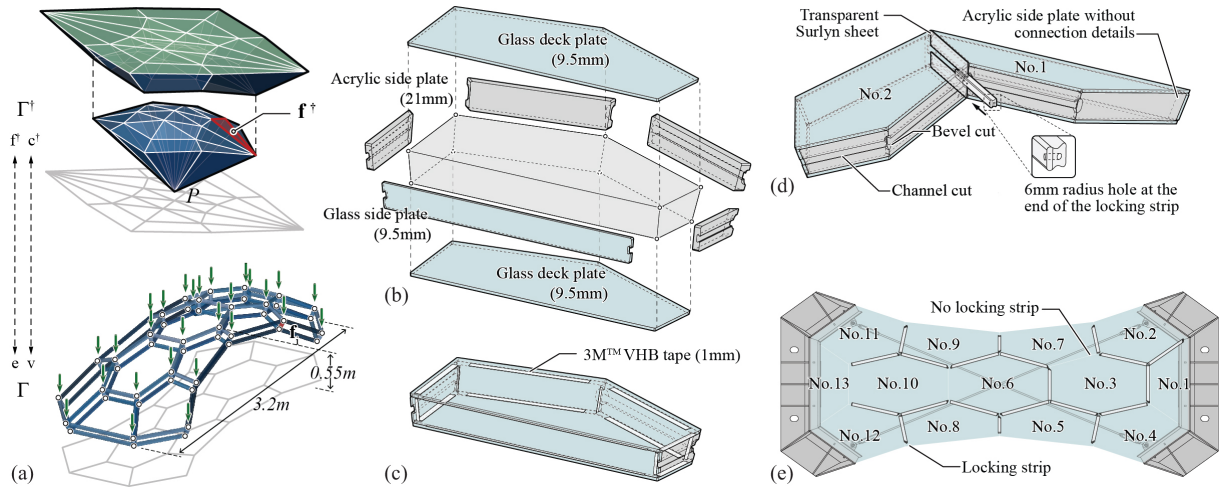


Figure 2. A graphic summary of the design, fabrication, and assembly of the glass bridge [5]. (a) The force and form diagram, (b) Glass deck plates and acrylic side plates in a typical HGU, (c) The plates are bonded using VHB tape, (d) Surllyn interface material and a locking strip are used to connect two neighboring HGUs, (e) The plan drawing of the bridge showing the locking strip layout.

The final assembly sequence is selected aiming for the least number of side plate pairs that cannot have butterfly connection, and eventually, twenty out of the total twenty-six HGU-to-HGU contacts are secured by the butterfly locking mechanisms (Figure 2e).

3. Numerical Analysis

In this section, first, the proposed strategy for numerically modeling the multi-layer sheet-based glass bridge is described. Next, different assumptions and steps of numerically modeling the bridge is explained.

3.1. Numerical Analysis Strategy

A micro-scale modeling strategy is proposed to accurately simulate the behavior of the designed multi-layer funicular sheet-based glass bridge model. This approach is essential, as it allows for the detailed representation of each component separately, crucial given the material heterogeneity in multi-layer structures where different layers react differently under stress. By focusing on the microstructural level, where individual parts exhibit distinct mechanical properties, this method enhances our understanding of how these variations and the bridge's complex geometry affect the overall structural behavior.

The primary focus of this modeling strategy is capturing the intricate interactions and complex geometric configurations between the different layers and components. These interactions are critical as they determine how loads are transferred and how components behave under real-world loading conditions, often involving significant deformations. If these interactions are not defined accurately, large displacements, specifically in contact areas, and the resulting nonlinear behaviors can lead to convergence issues in the model, complicating simulations and potentially leading to inaccurate predictions. Thus, accurately modeling these connections and the complex geometric details is essential for reflecting true structural behavior, particularly to prevent issues such as improper load transfer that can arise from these complexities. Moreover, the reliance on macro-structure strategies often proves inadequate in such scenarios because these broader approaches tend to overlook the detailed interactions that are cru-

cial in multi-layer configurations. Macro-structure strategies typically use generalized assumptions and average out the variations within complex structures, which can mask critical stress points and interactions that are vital for predicting failure modes and structural weaknesses, especially under dynamic and multi-dimensional loading conditions. This oversimplification is particularly problematic in structures like the multi-layer glass bridge, where understanding the specific behavior of each layer and junction is essential to ensure safety and performance.

By focusing on detailed, micro-scale interactions, the nonlinear behavior of materials, and the challenges of modeling complex geometries, this strategy aims to create a highly accurate simulation of the multi-layer funicular sheet-based glass bridge. Such a detailed approach ensures that the model not only mirrors the actual behavior under diverse conditions but also aids engineers in designing structures that are both safe and efficient. This precision is something that macro-structure strategies simply cannot provide, making them unsuitable for accurately predicting the complex dynamics of sophisticated architectural designs. The proposed micro-scale modeling strategy involves defining two distinct types of interactions based on different behavior occurring between different parts and the model's fabrication and construction process:

1. **Cohesive Interactions:** These interactions occur between surfaces bonded together using cohesive materials. This type of interaction accounts for the adhesive properties of the materials and the bonding process involved in the construction of the structure.
2. **Frictional Interactions:** These interactions occur between surfaces that are simply placed together without the use of adhesives. Frictional forces between these surfaces play a significant role in the overall behavior of the structure, influencing its stability and load transfer mechanisms.

Cohesive interactions cause sticky contact between adjoining surfaces, preventing relative movement due to cohesive material between them [3]. Surface-based tie constraints simplify defining these interactions by assuming perfect, motionless contact, but may lead to over-constraining issues. Alternatively, the cohesive zone model (CZM), based on the traction-separation law, more accurately depicts cohesive material behavior and crack propagation, simulating adhesive bonds between surfaces and sticky contacts. The two main CZM types are Element-Based CZM (ECZM), which uses a separate layer of cohesive elements, and Surface-Based CZM (SCZM), suitable for minimal thickness adhesive layers. The constitutive behavior of cohesive elements in ECZM can be modeled using continuum-based, traction-separation-based, or uniaxial stress-based methods, each suited for different material thickness and constraints.

Frictional interactions cause relative movements at contact points, producing normal and tangential stresses. These interactions are modeled using various finite element algorithms, including node-to-node, node-to-surface, and surface-to-surface discretizations. Node-to-node discretization imposes constraints between node pairs, making it suitable for linear geometries. Node-to-surface discretization, a nonlinear approach, imposes constraints between nodes and their nearest projection points on the opposing surface. Surface-to-surface discretization approximates these constraints across entire surfaces. To define these interactions, the penalty method is often used, which implements the Coulomb friction model. This model relates the maximum allowable frictional (shear) stress to the contact pressure before sliding occurs. The Coulomb friction model defines the critical shear stress by the coefficient of friction, which must be set by the user, ideally based on experimental test data.

3.2. Numerical Modeling

In this section, different steps of the modeling process are explained.

Interactions: The critical aspect of the proposed methodology lies in the selection and definition of interactions among the components of the multi-layer sheet-based glass bridge. By analyzing the role and impact of each component within the overall model, various interactions are defined. Additionally, the assembly sequence during fabrication and construction significantly influences the model’s behavior. Consequently, different cohesive and frictional interactions are specified based on these considerations, as follows:

1. **Interaction Between HGUs and VHB Tapes: Cohesive** Given the non-negligible thickness of these tapes, cohesive elements based on the ECZM are used to model the adhesive interactions. Additionally, the constitutive behavior of these tapes is defined as a continuum.
2. **Interaction Between HGUs bonded to Primary Interface Surfaces: Cohesive** Based on the assembly sequence described, primary interface surfaces are initially attached to an HGU by adhering them to the neighboring side plates of the HGUs using adhesive gorilla spray. Since the adhesive gorilla spray lacks thickness, the interaction between the glass and interface materials is characterized as cohesive behavior, defined according to the SCZM.
3. **Interaction Between HGUs and Secondary Interface Surfaces: Frictional** For all other sides of interface materials that are not initially bonded to an HGU and are positioned between HGUs, a frictional interaction occurs between the side plates, interface materials, and glass sheets. This type of interaction is governed by the Coulomb friction law and is characterized as a surface-to-surface friction-based interaction with a coefficient of friction set at 0.4
4. **Interaction Between Side Plates and Locking Bars: Frictional** Since side plates are simply placed between each other, a surface-to-surface friction-based interaction is established. This interaction is governed by the Coulomb friction law and features a coefficient of friction of 0.4.

Material Properties: Accurately defining material properties is essential in Finite Element Analysis to ensure models reflect actual physical behavior. Precisely defining mechanical properties like Young’s modulus and Poisson’s ratio are critical and should be based on testing data relevant to the materials and processes used, as inaccuracies in these properties can lead to misleading results. In the model, both the glass and acrylic materials are modeled as linearly-elastic due to their behavior under typical load conditions. Surlyn sheets, which normally exhibit elastic-plastic properties, are simplified to elastic materials in the model to avoid unnecessary complexity, as they remain within the elastic range under study loads. Their properties are sourced from the Dow Company’s technical data sheet. For VHB tapes, which are viscoelastic, a hyperelastic approximation is used based on Uniaxial Tension test data from 3M company, which is illustrated in Figure3. This simplification is considered adequate for the simulation’s scope and expected to provide reliable results. The mechanical properties for all materials are summarized in Table1.

Table 1. Defined material properties.

Material	Density (kg/m ³)	Young’s Modulus (MPa)	Poisson’s Ratio
Glass	3000	70000	0.2
Acrylic	1500	3000	0.37
Surlyn	1500	350	0.4

Mesh: Meshing a model effectively requires careful consideration of element types and mesh size. Research has shown that hexahedral elements often yield more accurate simulations than tetrahedral

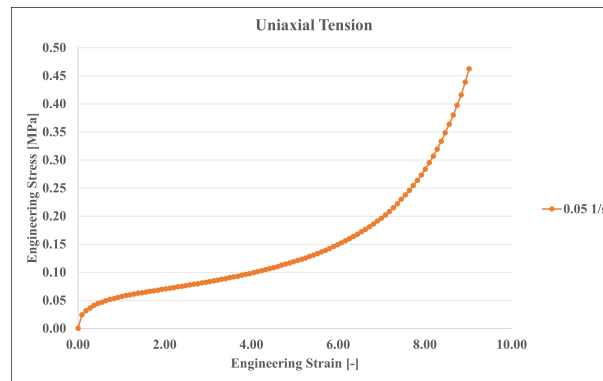


Figure 3. The experimental uniaxial tension test data by Dow company

elements due to the latter's tendency to increase stiffness. However, complex geometries, such as those found in side plates and locking bars, may necessitate the use of tetrahedral elements. Moreover, while second-order elements enhance simulation accuracy, they also significantly raise computational costs. In contrast, first-order elements, though less costly, can introduce issues like shear-locking or hour-glassing in bending scenarios. Through trial-and-error, it was determined that linear elements, despite their lower computational demands, do not compromise the simulation's outcomes significantly. Consequently, all parts are meshed with linear elements, but with varying types depending on their specific requirements, mainly the geometry. Mesh size selection is another critical factor, balancing desired accuracy with computational efficiency. A mesh sensitivity analysis helps identify an optimal size that achieves sufficient accuracy without undue computational burden. For this model, mesh sizes were also determined through trial-and-error, aiming to balance accuracy and cost. Specifically, linear hexahedral elements were used for glass and surlyn interfaces, while the more complex shapes of locking bars and acrylic side plates required linear tetrahedral elements. Additionally, cohesive elements were employed for VHB tapes as discussed in previous sections.

Loading and Boundary Conditions: In the modeling process, the steel abutment was not considered. Nevertheless, the boundary conditions of the supports were simplified, and a pinned connection was applied all over glass surfaces at the two ends. The loading was applied by utilizing the displacement-control approach. Similar to the experimental setup, the loading was applied on the top of two adjoining lines of the middle HGU with its right and left HGUs by utilizing the displacement-control approach. The loading and boundary conditions can be seen in Figure4.

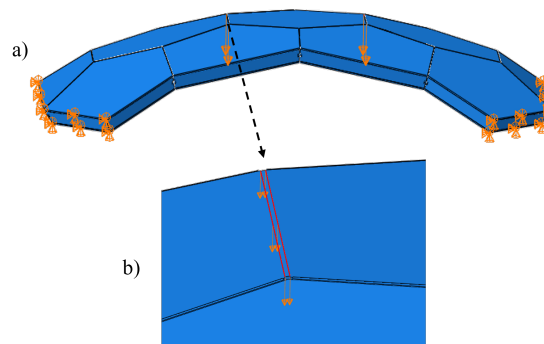


Figure 4. Loading and boundary condition modeling, a) an overall view, b) detailed view of applied loading

4. Experimental verification

To evaluate the numerical model, a 3.3 m span prototype bridge was tested under symmetrical and asymmetrical load conditions. The bridge, supported by steel abutments bolted to a strong floor and reinforced with two 'X' shaped tension ties across the abutments, was subjected to a maximum symmetric load of 7.1 kN on the left and right joints of the middle unit (HGU-6), and maximum asymmetric load of 4.68 kN only on one joint of HGU-6 using a hydraulic actuator. The symmetric load simulates a 4.0 kN/m² pedestrian live load across all centerline top deck plates, indicative of the bridge's service limit state behavior. Displacements were monitored using potentiometers placed at the southern, northern, and central points of the HGUs, details of which are shown in Figure 5. Notably, the joint between HGU-2 and HGU-6 lacked a locking bar, unlike the connection between HGU-6 and HGU-7.

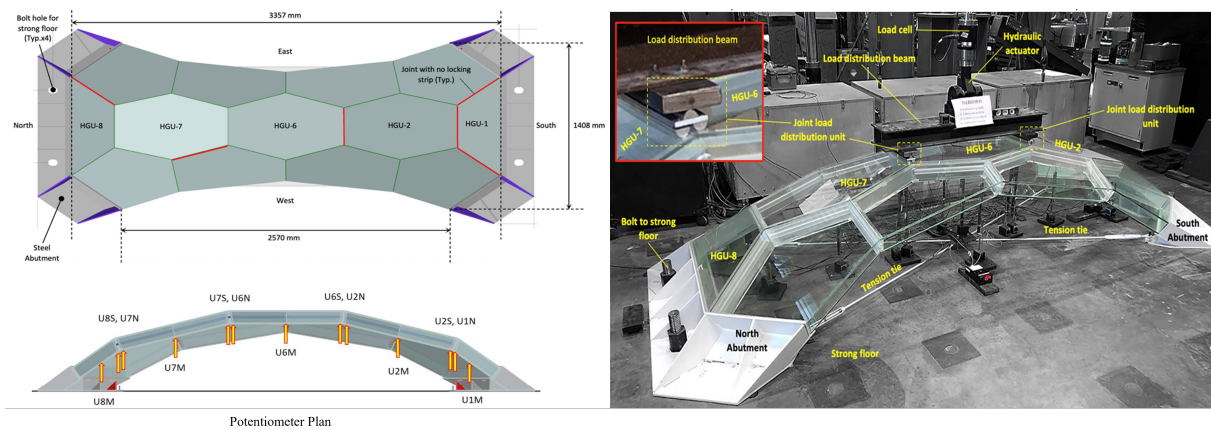


Figure 5. Details of the test setup.

Experimental tests on the bridge prototype under symmetric load revealed a maximum displacement of 6.5 mm on both sides of the middle unit (HGU-6), well below the allowable limit of 9 mm ($L/360$) for unfactored pedestrian live loads. The central span displacement was 4.35 mm, 20% less than at the sides, likely due to second-order bending effects in the bottom deck plate, causing flexural buckling and compression on the outer surface of the bottom deck plate. Under the asymmetric loading, the maximum displacement of 9.22 mm was measured for the south side of the middle unit (HGU-6).

The numerical model was simulated under symmetric and asymmetric loading condition for static analysis, and displacements were measured at specific points on each HGU where potentiometers were placed in the experimental setup. Figure 6c and Figure 7c compares these displacements with experimental results under symmetric and asymmetrical loading, respectively, showing a close alignment in the overall displacement trends, including points of uplift or push. Despite some instances where the simulated model shows lower displacement, indicating higher stiffness, the maximum deviation from the experimental model is around twice, highlighting the effectiveness and accuracy of the proposed methodology. This methodology has demonstrated superior accuracy over other simulated models tested with different approaches, particularly due to the precise incorporation of the assembly sequence and interactions between interface materials and other components. Previous test models that neglected these considerations displayed a stiffness seven times greater than the actual bridge, underscoring the critical role of detailed modeling in achieving realistic simulation results.

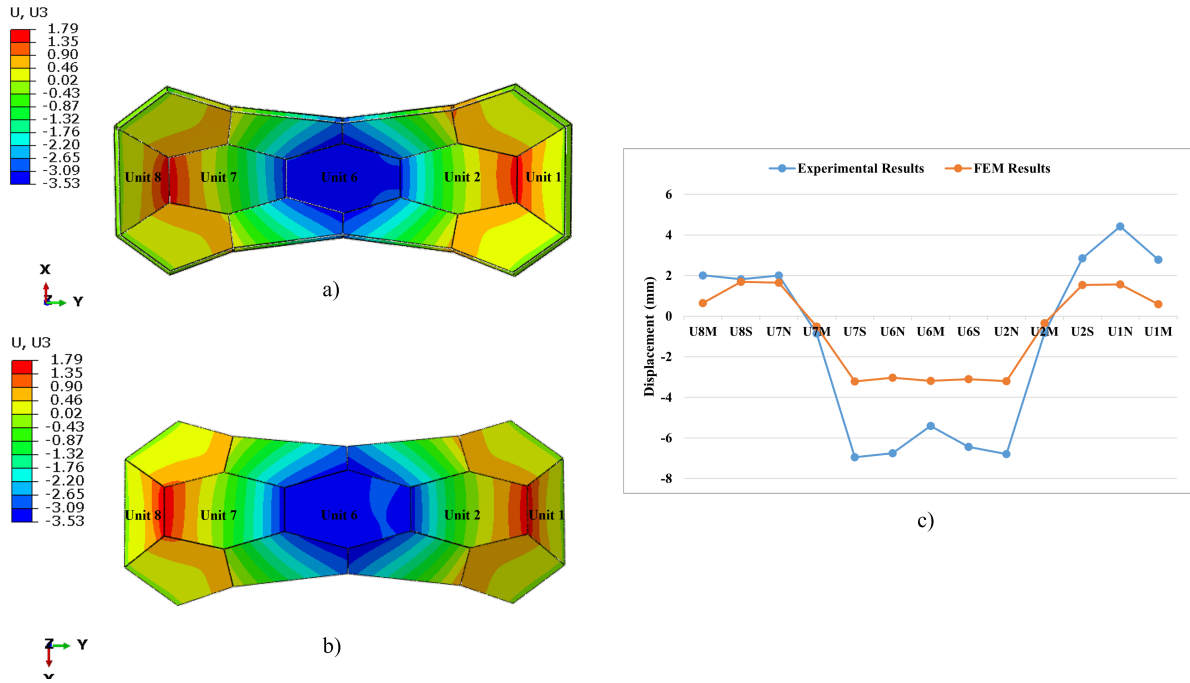


Figure 6. The final results of the numerical analysis modeling under symmetric loading of 7.1 kN. (a) Displacements of glass sheets from the top view, (b) Displacements of glass sheets from the bottom view, (c) a comparison between experimental and numerical results of displacements at different points on HGUs according to the locations of potentiometers in the experimental setup; positive displacements show uplift, while negative displacements show push on the bridge.

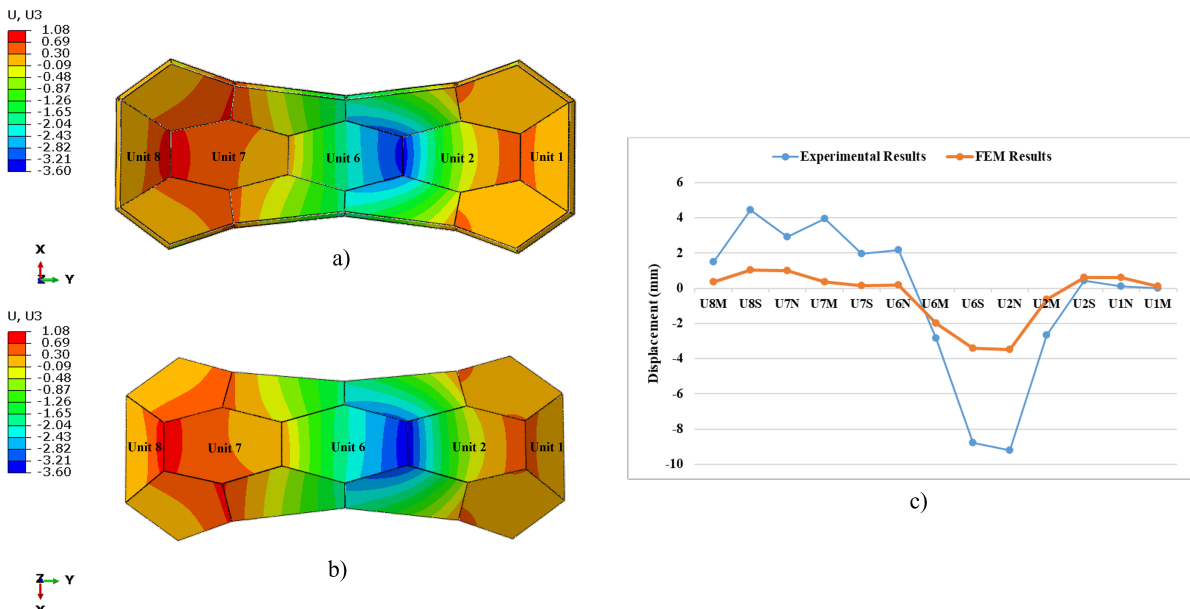


Figure 7. The final results of the numerical analysis modeling under asymmetric loading of 4.68 kN. (a) Displacements of glass sheets from the top view, (b) Displacements of glass sheets from the bottom view, (c) a comparison between experimental and numerical results of displacements at different points on HGUs according to the locations of potentiometers in the experimental setup; positive displacements show uplift, while negative displacements show push on the bridge.

5. Conclusion

The analysis results of the proposed method on a multi-layer funicular glass bridge prototype are compared and verified by experimental laboratory testing under different loading scenarios and have shown reasonable agreement with measured experimental behavior. The model is comprehensive and therefore could be used for modeling any multi-layer sheet-based structure.

Acknowledgments

This research was partially supported by the National Science Foundation Future Eco Manufacturing Research Grants NSF, FMRG-2037097 CMMI and NSF CAREER-1944691 CMMI.

References

- [1] J. Peng and X. Li, "A numerical simulation of the seismic performance and residual stress of welded joints in building steel structures based on the finite element method," *Processes*, vol. 12, no. 2, p. 263, 2024.
- [2] F. Dashti, R. P. Dhakal, and S. Pampanin, "Numerical modeling of rectangular reinforced concrete structural walls," *Journal of structural engineering*, vol. 143, no. 6, p. 04017031, 2017.
- [3] M. Bolhassani, A. A. Hamid, A. C. Lau, and F. Moon, "Simplified micro modeling of partially grouted masonry assemblages," *Construction and Building Materials*, vol. 83, pp. 159–173, 2015.
- [4] F. Yavartanoo and T. H.-K. Kang, "Dry-stack masonry wall modeling using finite-element method," *Journal of Structural Engineering*, vol. 148, no. 11, p. 04022176, 2022.
- [5] Y. Lu, A. Seyedahmadian, P. A. Chhadeh, M. Cregan, M. Bolhassani, J. Schneider, J. R. Yost, G. Brennan, and M. Akbarzadeh, "Funicular glass bridge prototype: Design optimization, fabrication, and assembly challenges," *Glass Structures & Engineering*, vol. 7, no. 2, pp. 319–330, 2022.
- [6] M. Bolhassani, C. Byrnes, and J. R. Yost, "Behavior of modular components in a funicular glass bridge."
- [7] S. Hussain, P. S. Chen, D. Hassanlou, M. Bolhassani, and C. Bedon, "Bending and lateral-torsional buckling investigation on glass beams for frameless domes," *Results in Engineering*, p. 101962, 2024.
- [8] Y. Lu, A. Seyedahmadian, P. A. Chhadeh, M. Cregan, M. Bolhassani, J. Schneider, J. R. Yost, G. Brennan, and M. Akbarzadeh, "Tortuca: An ultra-thin funicular hollow glass bridge," in *The Projects Catalog of the 42nd Annual Conference for the Association for Computer Aided Design in Architecture (ACADIA)*, Philadelphia, PA, Oct. 2022, pp. 166–171.
- [9] Y. Lu, M. Cregan, P. Chhadeh, A. Seyedahmadian, M. Bolhassani, J. Schneider, J. Yost, and M. Akbarzadeh, "All glass, compression-dominant polyhedral bridge prototype: Form-finding and fabrication," in *Proceedings of the 7th International Conference on Spatial Structures and the Annual Symposium of the IASS*, Surrey, UK, Aug. 2021, pp. 326–336.
- [10] PSL, *PolyFrame*, <https://www.food4rhino.com/app/polyframe>, Aug. 2018. [Online]. Available: <https://www.food4rhino.com/app/polyframe>.
- [11] A. Nejur and M. Akbarzadeh, "Polyframe, efficient computation for 3d graphic statics," *Computer-Aided Design*, vol. 134, p. 103003, 2021.